NASA CONTRACTOR REPORT

NASA CR-2627

NASA CR-2627

DIFFERENTIAL ABSORPTION AND SCATTERING SENSITIVITY PREDICTIONS

Richard T. Thompson, Jr.

Prepared by
OLD DOMINION UNIVERSITY
Norfolk, Va. 23508
for Langley Research Center

NATIONAL AERONAUTICS AND SPACE ADMINISTRATION • WASHINGTON, D. C. • AUGUST 1976

1. Report No.	2. Government Accession No.	3. Recipient's Catalog No.
NASA CR-2627		

4. Title and Subtitle	5. Report Date
DIFFERENTIAL ABSORPTION AND SCATTERING SENSITIVITY PREDICTIONS	August 1976
	6. Performing Organization Code

7. Author(s)	8. Performing Organization Report No.
Richard T. Thompson, Jr.	PGSTR-PH75-19
	10. Work Unit No.
	645-20-01-01

9. Performing Organization Name and Address	11. Contract or Grant No.
Department of Physics and Geophysical Sciences Old Dominion University Norfolk, Virginia 23508	NSG 1060
	13. Type of Report and Period Covered Contractor Report June 1974 - November 1975
12. Sponsoring Agency Name and Address	14. Sponsoring Agency Code
National Aeronautics and Space Administration Washington, D.C. 20546	

15. Supplementary Notes
This contract was monitored by the Environmental and Space Sciences Division of Langley Research Center. For additional information, contact Ellis E. Remsberg, Langley Research Center, Mail Stop 401A, Hampton, Virginia 23665. Topical Report

16. Abstract

A set of general equations for evaluating the sensitivity of the Differential Absorption and Scattering (DAS) technique based upon a conventional analysis of statistical errors is derived in this report. The equations are put in a proper form for evaluating total column density and range resolved concentration measurements of a variety of atmospheric species. The derived equations are subsequently used to analyze the sensitivity of DAS in three specific applications assuming realistic parameters for the optical and electronic components of proposed DAS systems.

The three DAS applications evaluated are: (1) measurement of nitrogen oxide (NO_2) at ground levels over a horizontal path, (2) measurement of atmospheric ozone (O_3) depletion in the wake of a jet engine at 20 km altitude, and (3) measurements of the ozone distribution in the atmosphere from an orbiting space platform, in a downward viewing mode. The results of this study have shown that with reasonable laser energy and telescope receiver dimensions, DAS is capable of meeting requirements for performing these measurements.

17. Key Words (Suggested by Author(s))	18. Distribution Statement
Laser Radar Air Pollution Differential Absorption	Unclassified - Unlimited Subject Category 45

19. Security Classif. (of this report)	20. Security Classif. (of this page)	21. No. of Pages	22. Price*
Unclassified	Unclassified	41	$3.75

* For sale by the National Technical Information Service, Springfield, Virginia 22161

TABLE OF CONTENTS

LIST OF TABLES

LIST OF FIGURES

I. SUMMARY

A set of general equations for evaluating the sensitivity of the Differential Absorption and Scattering (DAS) technique based upon a conventional analysis of statistical errors is derived in this report. The equations are put in a proper form for evaluating total column density and range resolved concentration measurements of a variety of atmospheric species. The derived equations are subsequently used to analyze the sensitivity of DAS in three specific applications assuming realistic parameters for the optical and electronic components of proposed DAS systems.

The three DAS applications evaluated are: (1) measurement of nitrogen dioxide (NO_2) at ground levels over a horizontal path, (2) measurement of atmospheric ozone (O_3) depletion in the wake of a jet engine at 20 km altitude, and (3) measurements of the ozone distribution in the atmosphere from an orbiting space platform, in a downward viewing mode. The results of this study have shown that with reasonable laser energy and telescope receiver dimensions, DAS is capable of meeting requirements for performing these measurements.

II. INTRODUCTION

Differential Absorption and Scattering (DAS) is a single ended active remote sensing technique for monitoring concentration of various atmospheric gases. Since DAS relies on Rayleigh and Mie backscatter, ranging information is possible. The technique was first applied by Schotland (1965)[1] to determine the vertical profile of atmospheric water vapor using a ground based ruby laser which was tuned through a water vapor absorption line. Although a detailed uncertainty analysis was not performed for this early measurement, a signal-to-

noise ratio for the return signals was estimated and standard deviations were obtained for sets of measurements. The results of this early measurement did show a trend of increasing cumulative water vapor with altitude as expected. A recent report of Measures (1971)[2] illustrates the advantages of differential absorption to either Raman Scattering or Resonant Fluorescence. This result is expanded in a later report by Measures and Pilon (1972)[3] but no detailed sensitivity expression was derived.

Kildal and Byer (1971)[4] presented details of comparison for Raman backscatter, resonance backscatter, and resonance absorption. The resonance absorption considered requires a remote detector on a retroreflector and does not include the phenomena of molecular or aerosol backscatter utilized in DAS measurements. The DAS concept was included in a later report of Byer and Garbuny (1973).[5] Other aspects of an error analysis of the DAS (or DASE for Differential Absorption of Scattered Energy) are presented by Schotland (1974)[6] and Ahmed (1973).[7] In the work presented here a more basic approach was used than in the earlier works and the analysis is developed around the concept of a system that measures energy (or photons) rather than power with a given bandwidth. The measurability criteria or sensitivity used in this report is a predicted standard deviation based upon Gauss and Poisson statistics. A percentage predicted uncertainty is expressed by dividing the propagated standard deviation by the "measured" value. There is a 67% probability that a single measurement of a given quantity (defined as the signal S in signal-to-noise S/N) will fall within one standard deviation (the noise N) of its true value. The expressions derived in this report have been incorporated into a DAS simulation computer program developed by Stanford Research Institute in order to more justifiably predict the retrievability of pollutant profiles in the atmosphere. The equations derived allow one to determine the sensitivity of measuring a

gas concentration as determined by limitations of background noise, attenuation due to factors other than the gas of interest and backscattering variations.

III. THE DIFFERENTIAL ABSORPTION AND SCATTERING TECHNIQUE

The concept of differential absorption and scattering is illustrated in the case treated by Byer and Garbuny[5] shown here as Figure 1 through Figure 3. A laser beam is encompassed by the field of view of the telescope as shown in Figure 1. The cloud at the center of Figure 1 represents a gaseous plume for which a concentration measurement is desired. Two range cells corresponding to detector gate time intervals T_j and T_{j+1} at ranges R_j and R_{j+1} contain Rayleigh and Mie scatterers such that backscattered laser light plus background (e.g., scattered sunlight) are received at the detector situated at the focal point of the telescope. The ΔR_j shown in Figure 1 represents the spatial range over which a difference in column content applies in determining concentration as a function of range. The expected return signal is plotted in Figure 2 as a function of range for the strongly absorbed signal S_1 and the weakly absorbed signal S_2. Note that the R^2 dependence has been removed from the return signal profiles.

The logarithm of the return signals $\text{Log}_e[S_1/S_2]$ at each wavelength is plotted as M in Figure 3 illustrating the column content as a function of range under conditions of identical losses at both wavelengths due to materials other than the particular gas of interest.

Finally, the curve labeled as N in Figure 3 depicts the constituent (in this case a pollutant) gas concentration as a function of range as obtained by differentiating M with respect to range R. The precision with which concentration can be determined is a function of the noise on the signal return and the range resolution or averaging time T_j required.

A. The Lidar Equation

In this section an expression for the backscattered signal is defined for a DAS system in terms of atmospheric and system parameters. The Lidar return signal strength S_{ij} observed at the detector from range cell j at range R_j for wavelength λ_i is given in photons per range cell (for $Q = 1$) by*

$$S_{ij} = \frac{QU_i}{h\nu_i} \frac{A}{R_j^2} \frac{B_{ij}\, cT_j}{2} T_s \, \mathrm{EXP}\left\{-2\int_0^{R_j} [\xi_i(r) + N(r)\alpha_i(r)]\, dr\right\} + Qn_{iD} + Qn_{iB} \tag{1}$$

where

- Q represents electronic amplification which converts photons received per range cell (T_j) to charge stored by electronics;
- U_i is the energy of the laser pulse at wavelength λ_i, joules;
- h is Planck's constant, joule-sec;
- A is the effective area of the receiver telescope, m^2;
- R_j is the range at which the j^{th} range cell is located, m;
- B_{ij} is the combined Rayleigh and Mie backscattering coefficient at wavelength λ_i in range cell j, $m^{-1}\ sr^{-1}$;

---

* It is assumed that

$$S_{ij} = 2\int_a^b \left[\frac{S_i'}{cT_j}\right] dr$$

where

$$a = R_j - \frac{cT_j}{4},$$

$$b = R_j + \frac{cT_j}{4},$$

and S_i' is the backscattered laser signal at wavelength λ_i from range r observed at the lidar receiver. This assumption requires that the average return signal strength from range cell j can be represented by the return signal strength calculated at the midpoint of the cell.

c is the speed of light, m/sec;

T_j is the integration or gate time for the detector, corresponding to a range cell at R_j, sec;

T_s is the optical efficiency of the telescope-filter-detector system at wavelength λ_i;

$\xi_i(r)$ is the extinction due to interferents such as Rayleigh scattering, Mie scattering and atmospheric constituents other than those included in $N(r)\alpha_i(r)$ at wavelength λ_i and range r, m^{-1};

$N(r)$ is the concentration of atmospheric constituent gas to be measured, atm;

$\alpha_i(r)$ is the photo-absorption coefficient at wavelength λ_i, $(\text{atm cm})_e^{-1}$

n_{iD} is the equivalent number of photons counted due to the detector dark current during time T_j, photons;

n_{iB} is the equivalent number of photons counted due to background such as scattered sunlight, photons.

The return signal strength due only to backscattered laser light is obtained by subtracting the background and detector noise levels defined as

$$S_i = Q(n_{iD} + n_{iB}) \tag{2}$$

from the return signal strength of Equation (1). The Lidar equation evolves by subtracting Equation (2) from Equation (1) and dividing by the electronic amplification factor Q to obtain

$$n_{ij} = \frac{U_i \lambda_i A \beta_{ij} T_j T_{si}}{2hR_j^2} \text{ EXP} \left\{ -2 \int_o^{R_j} [\xi_i(r) + N(r)\alpha_i(r)] \, dr \right\} \tag{3}$$

where n_{ij} is photons per range cell resulting only from backscattered laser photons.

B. The Column Content Measurement

The column content of a given gas is defined here as the integral of gas concentration over a specified distance. For example, a molecular pollutant having a uniformly distributed density of N atmospheres (1 atmosphere = 2.69×10^{19} molecules $/ cm^3$) has a column content over a range of 1 meter given by 100 N atm cm or over a range of 1 km given by 10^5 N atm cm.

The column content M_j of a gas to range R_j can be obtained by measuring n_{1j} at λ_1 (on the absorption peak) and n_{2j} at λ_2 (off the absorption peak) and solving the ratio of n_{1j} to n_{2j} of Equation (3) for the integrated concentration (assuming a constant difference in absorption coefficient) to obtain:

$$M_j = \int_o^{R_j} N(r)dr$$

$$= \frac{1}{2(\alpha_1 - \alpha_2)} \left\{ \text{Log}_e \frac{n_{2j} U_1}{n_{1j} U_2} + \text{Log}_e \frac{\beta_{1j} T_{s1} \lambda_1}{\beta_{2j} T_{s2} \lambda_2} - 2\int_o^{R_j} [\xi_1(r) - \xi_2(r)]\, dr \right\}. \tag{4}$$

The dominant term of this calculation must be $\text{Log}_e(n_{2j}\, U_1/n_{1j}\, U_2)$ for any measurement so as to minimize the requirement of a precise a priori knowledge of the other terms. Requirements on precision and resulting limitations are discussed in a following section. The column content as expressed by Equation (4) is valid also when a retroreflector is used where β_{1j}/β_{2j} is replaced by the ratio of reflectivity at the two wavelengths.

In terms of the measured parameters S_{ij}, S_i, and U_i Equation (4) becomes:

$$M_j = \frac{1}{2(\alpha_1 - \alpha_2)} \left\{ \text{Log}_e \frac{(S_{2j} - S_2)\, U_1}{(S_{1j} - S_1)\, U_2} + \text{Log}_e \frac{\lambda_1 \beta_{1j} T_{s1}}{\lambda_2 \beta_{2j} T_{s2}} - 2\int_o^{R_j} [\xi_1(r) - \xi_2(r)]\, dr \right\}. \tag{5}$$

In developing equations (4) and (5) it is assumed that photo-absorption has no r dependence which is not necessarily true such as when atmospheric pressure

or temperature changes with r. When this approximation is not valid the properties of the measurement path must dictate how α_1 and α_2 will be determined as weighted averages. An alternative would be to express "pollutant" level as an optical depth difference (i.e., $\int_0^R N(r)[\alpha_1(r) - \alpha_2(r)]dr$) which is readily obtained from Equation (3).

C. The Range Resolved Concentration Measurement

The concentration of an atmosphere constituent can be determined as a function of range by dividing the difference in column content at two ranges by the difference in the respective ranges. The resulting measure of concentration will represent a mean over the range increment involved and will have a range position determined as the mean range.

The average concentration $\langle N \rangle_j$ contained in a range increment R_j to R_{j+1} is defined as

$$\langle N \rangle_j = \frac{1}{R_{j+1} - R_j} \int_{R_j}^{R_{j+1}} N(r)dr = \frac{1}{R_{j+1} - R_j} (M_{j+1} - M_j) \ . \tag{6}$$

Then from Equation (5) it follows that

$$\langle N \rangle = \frac{1}{2\Delta\alpha\Delta R_j} \left\{ \underbrace{\mathrm{Log}_e \left[\frac{(S_{2j+1} - S_2)(S_{1j} - S_1)}{(S_{1j+1} - S_1)(S_{2j} - S_2)} \right]}_{(A)} + \underbrace{\mathrm{Log}_e \frac{\beta_{1j+1}\beta_{2j}}{\beta_{2j+1}\beta_{1j}}}_{(B)} \right.$$
$$\left. \underbrace{- 2 \int_{R_j}^{R_{j+1}} [\xi_1(r) - \xi_2(r)]dr}_{(C)} \right\} \tag{7}$$

where

$$\Delta\alpha = \alpha_1 - \alpha_2$$

and

$$\Delta R_j = R_{j+1} - R_j$$

The values of term (A) are of primary importance for an uncertainty analysis since they are the largest determining factor of Equation (7) whereas the values

in (B) will exactly cancel when Rayleigh scattering dominates or when Mie scattering dominates in both range cells j and $j+1$. The values in the (C) term represent other loss mechanisms and must be included for completeness. Limitations due to terms (B) and (C) are discussed below.

IV. PREDICTIONS OF DAS SENSITIVITY

An estimate of uncertainty, therefore sensitivity, of a DAS measurement can be obtained by use of the principle of least squares. Error propagation by least squares is treated by Bevington (1969)[8] and other standard texts on statistics and error analysis. The least square procedure is described briefly below. Assume a normal distribution of error δX_i (the standard deviation) about the true value X_i of a set of n measured parameters describing a function $f(X_1 \ldots X_n)$. Consider a Taylor expansion of f about the mean values of each X_i; square $f - f_o$; average over a large number N of observations to eliminate odd order terms, then drop fourth order and higher terms to obtain the error propagation form of least squares

$$[\delta f(X_1 \ldots X_n)]^2 = \sum_{i=1}^{n} \left[\left(\frac{\partial f}{\partial X_i}\right)^2 (\delta X_i)^2\right] \tag{8}$$

where

$$\delta f(X_1 \ldots X_n) = \sqrt{\frac{\sum_{j=1}^{N} [f(X_1{}^j \ldots X_n{}^j) - f_o(X_{o1}{}^j \ldots X_{on}{}^j)]^2}{N - 1}}$$

and

$$\delta X_i = \sqrt{\frac{\sum_{j=1}^{N} [X_i{}^j - X_{oi}{}^j]^2}{(N - 1)}}$$

The zero subscript denotes mean value. The above definitions of δf and δX_i show their relation to variance and standard deviation. For purposes of uncertainty prediction the values of δX_i can be determined from Poisson

statistics, from standard deviations of measured data, or from other statistical arguments that fit a given situation.

A. Predicted Sensitivity in Column Content

The predicted uncertainty in column content δM_j is obtained by operating on Equation (4) with Equation (8) to obtain

$$\delta M_j = \left\{ \frac{1}{2\Delta\alpha} \left[\frac{(\delta S_{2j})^2 + (\delta S_2)^2}{(S_{2j} - S_2)^2} + \frac{(\delta S_{1j})^2 + (\delta S_1)^2}{(S_{1j} - S_1)^2} + \left(\frac{\delta U_1}{U_1}\right)^2 + \left(\frac{\delta U_2}{U_2}\right)^2 + \frac{(\delta(\beta_{1j}/\beta_{2j}))^2}{(\beta_{1j}/\beta_{2j})^2} + 4(\delta(\xi R)_j)^2 \right] + \frac{(\delta\Delta\alpha)^2}{(\Delta\alpha)^2} M_j^2 \right\}^{1/2} \quad (9)$$

The values of T_{S1} and T_{S2} are not subject to random fluctuations and are not included in Equation (9). The values of δS_{ij}, δS_i, $\delta(\beta_{1j}/\beta_{2j})$ and $\delta(\xi R)_j$ are discussed below. The value of $\delta(\Delta\alpha)$ is considered inconsequential for applications considered in this report but for other applications standard deviations of measured values may be required. The uncertainties in laser energy δU_i can be made inconsequential by design but are included in Equation (9) to indicate the precision with which U_i must be measured.

B. Predicted Sensitivity in Range Resolved Concentration

The predicted uncertainty in range resolved concentration measurement δN_j is obtained by operating on Equation (7) with Equation (8) where $f = \langle N \rangle_j$ to obtain

$$(\delta N_j)^2 = \left\{ \left(\frac{1}{2\Delta\alpha\Delta R_j}\right)^2 \left[\sum_{i=1}^{2} \sum_{k=j}^{j+1} \frac{(\delta S_{iK})^2 + (\delta S_i)^2}{(S_{iK} - S_i)^2} + \left(\frac{\delta\beta_j'}{\beta_j'}\right)^2 + 4(\delta\langle\xi R\rangle_j)^2 \right] + \left[\frac{\delta(\Delta\alpha)\ \langle N\rangle_j}{\Delta\alpha} \right]^2 \right\}. \quad (10)$$

The value of $\delta(\Delta\alpha)$ is again ignored in this report for the same reasons stated in the above section. Suitable assignments for the rest of the standard deviation terms will now be discussed.

C. Uncertainty in return signal measurements

The uncertainties in S_{ij} and S_i are obtained by operating with Equation (8) on S_{ij} and S_i as defined by Equations (1), (2), and (3) to obtain

$$(\delta S_{iK})^2 = Q^2[(\delta n_{iK})^2 + (\delta n_{iD})^2 + (\delta n_{iB})^2] + (\delta Q)^2 (n_{iK} + n_{iD} + n_{iB})^2 \quad (11)$$

and

$$(\delta S_i)^2 = Q^2[(\delta n_{iD})^2 + (\delta n_{iB})^2] + (\delta Q)^2 (n_{iD} + n_{iB})^2 \quad (12)$$

The δ's of Equations (9), (10), (11), and (12) represent standard deviations from the mean. The standard deviations in laser backscatter δn_{ik} is assumed to be Poisson such that $\delta n_{ik} = \sqrt{n_{ik}}$ and can be calculated for an assumed laser lidar system and gas constituent profile from Equation (4). The value of δn_{iD}, the noise resulting from the detector varies from 0 (with respect to one photon per range cell) for a cooled photomultiplier to a value determined by[9]

$$(\delta n_{iD})^2 = \frac{(NEP)^2}{h^2\nu_i^2} T_j^2 = \frac{AT_j}{D^{*2}h^2\nu_i^2} \quad (13)$$

for a solid state detector. The noise equivalent power (NEP) is a parameter determined by the selected detector. The value of NEP depends upon the active surface area A, time response T_j and detectivity D* of the selected detector. Typical values of D* are on the order[10] of 10^{10} w^{-1} cm $sec^{-1/2}$ whereas the theoretical limit can be as high as 10^{13} at 3.0 μ (see, for instance, Putley[9]).

The noise generated from background fluctuations are assumed to be related to the background n_{iB} by Poisson statistics. For a system opto-electronic efficiency η, telescope field of view θ^2, telescope receiver area A, detector gate time T_j, spectral bandpass $\Delta\lambda_i$, and a spectral radiance B_r in w m^{-2} sr^{-1} nm^{-1} the received photon flux from the sky background is[2]

$$(\delta n_{iB})^2 = n_{iB} = \frac{\eta\pi\theta^2 AT_j\Delta\lambda_i B_r}{h\nu_i} \quad (14)$$

Values of B_r for the region 300.0 nm to 420.0 nm have been reported by Knestrick and Curcio[11] and range up to 9×10^{-2} w m^{-2} sr^{-1} nm^{-1}.

Uncertainties introduced by electronic amplification factor Q will depend upon the selected system. Specific knowledge of Q is not required since all terms containing it can be expressed in terms of $\delta Q/Q$. Typical values of $\delta Q/Q$ can range from <1% for a gated integrator coupled to an analog-to-digital converter to 2.3% for a logarithmic amplifier.

D. Uncertainty in Backscatter

Backscatter results from a sum of the Rayleigh and Mie backscatter which vary with λ^4 and λ^α $(1 \leq \alpha \leq 4)$, respectively, ignoring resonances. The value of β_{1j}/β_{2j} becomes a limiting factor in the calculation of column content M_j if the absolute value of $3\ \mathrm{Log}_e(\lambda_1/\lambda_2)$ is on the order of $2M_j\Delta\sigma$. Laser wavelengths should be chosen carefully so as to maximize $2M_j\Delta\alpha - 3|\mathrm{Log}_e(\lambda_1/\lambda_2)|$ while maintaining δM_j of Equation (9) within acceptable limits. It is possible to correct for this difference in backscattering between wavelengths to some degree of precision as indicated by the form of Equation (4). The value of $\delta(\beta_{1j}/\beta_{2j})$ must now reflect the precision to which the backscattering is known to be non-Rayleigh when a Rayleigh scattering relationship is assumed. The amount of Mie scattering can be estimated from visibility by the technique of Fenn.[12]

When a retroreflector is used the value of $\delta(\beta_{1j}/\beta_{2j})$ must reflect the precision to which the wavelength dependence of the retroreflector is known.

For range resolved measurements the limitations due to backscattering are in general less severe due to the self-cancelling nature as seen by inspection of Equation (7). The value of the (B) term is exactly zero if the backscatter wavelength dependence is unchanged between range cells j and j+1. This condition will exist if scattering is dominated by Rayleigh scattering or by

Mie scattering (with identical wavelength dependence) in both range cells. When backscattering of Rayleigh and Mie scattering or the wavelength dependence of Mie scattering (for the Mie dominant case) varies between range cells j and $j+1$ the value of term (B) of Equation (7) will be non-zero. Under this latter condition the value of $\delta\beta_j'/\beta_j'$ must reflect the precision to which $(\beta_{1\ j+1}\ \beta_{2j})/(\beta_{2\ j+1}\ \beta_{1j})$ is known. Under the conditions for which term (B) of Equation (7) is zero the value of $\delta\beta_j'/\beta_j'$ must reflect the precision to which identical wavelength dependence of scattering in range cell j and range cell $j+1$ is known.

E. Uncertainty in Extinction

The column content measurement as obtained via Equation (5) is limited when extinction due to secondary mechanisms such as absorption and scattering by other gases becomes comparable to the term containing the return signals The effects of these other mechanisms are reflected in the $\xi_1(r) - \xi_2(r)$ term in Equation (5) and can be systematically corrected when known. When this systematic correction $(\xi_1(r) - \xi_2(r))$ is required the measurement limitation becomes dependent upon the precision with which this correction can be determined as reflected in the $\delta(\xi R)_j$ term of Equation (9). In the case of column content measurements the correction applies to the entire column, whereas for the range resolved concentration measurement it applies only in the range increment ΔR_j in which the concentration is being determined.

The required systematic correction for secondary loss mechanisms in range resolved concentration measurements is contained in Equation (7) term (C) and becomes important when term (C) is comparable to term (A) containing the return signal strengths. The precision to which $\xi_1(r) - \xi_2(r)$ is determinable then becomes the limiting factor in measuring $\langle N\rangle_j$ as reflected by $\delta\langle\xi R\rangle_j$ in Equation (10).

If secondary losses result primarily from another gas the value of $\delta\langle\xi R\rangle_j$ is expanded in terms of the gas concentration and cross section uncertainties. If the limitation is due to aerosol or Rayleigh scattering the $\delta\langle\xi R\rangle_j$ must be evaluated in terms of the precision to which the scattering is known. For purposes of modeling, estimates of atmosphere constituency can be obtained from Elterman,[13,14] McCormick,[15] McClatchey, et al.,[16] and NASA publication SP-285.[17]

The results presented in the following section evaluate feasibility in terms of backscattered signal strength only in a pure Rayleigh atmosphere and do not consider backscatter limitations or extinction from secondary mechanisms. These considerations should be included as the next degree of sophistication.

V. RESULTS

A. Nitrogen Dioxide Measurements at Ground Level

The configuration used to determine predicted standard deviations for DAS measurements of NO_2 is the same as that described in Section III. In this section a parametric study is included, the object of which is to develop an intuitive concept for the impact of various experimental parameters on the measurement sensitivity. The absorption coefficients used are 17.9 $(\text{atm cm})_e^{-1}$ at 448.0 nm and 10.5 $(\text{atm cm})_e^{-1}$ at 446.0 nm as obtained from the resolved absorption spectra of Hall and Blacet[18] shown in Figure 4. A higher resolution absorption coefficient measurement could markedly increase the ranges of NO_2 concentrations considered as measurable by increasing $\Delta\alpha$ of Equation (9). The total Rayleigh-Mie extinction coefficient is taken as $\xi = 1.0 \times 10^{-4}\ m^{-1}$ whereas the backscatter coefficient is assumed as $\beta = 4.0 \times 10^{-6}\ m^{-1}\ sr^{-1}$ as suggested by Measures.[2] The detection system is assumed to have a 6-inch diameter telescope, an overall quantum efficiency of $T_s = .20$ and a detector gate window (or reciprocal bandwidth) of $T_j = 10$ ns. The laser power is assumed

to be 75 kW with a pulse width of 10 ns yielding an energy per pulse of $u_1 = u_2 = .75$ millijoule. A background intensity of $n_{1B} = n_{2B} = 100$ photons^2 per gate time is assumed for these calculations to represent daytime measurements. The above set of parameters is not intended to represent an optimized system but to provide a base from which an optimized system can be defined as described later.

The predicted standard deviation of an average concentration of NO_2 over range R is shown in Figure 5 for various ranges as a function of NO_2 concentration for the above conditions. From Figure 5 it is apparent that from a 10 ns range cell at 900 m the column content can be measured to no better than about 75% and then only at an average concentration of 1.1 ppm over the 900 m. The degree of sensitivity (predicted percent standard deviation) improvement is shown on Figure 5 as the distance from the LIDAR to the range cell decreases to 100 m showing a broadening of the measurable set of concentrations. At 100 m the return signals from the range cell are capable of determining the average NO_2 concentration to within 20% if it falls in the region of 1 to 45 ppm. In practice upper or lower limits can be set on an off-scale measurement by determining whether the predicted error is large due to strongly attenuated signals or a lack of signal differential, respectively. The predicted standard deviations are expected to improve for a night operation where the background would be zero. We can define a span of range and concentration within which meaningful measurements of total burden can be performed by setting Equation (9) equal to the required minimum of precision (say, $\Delta M/M = 20\%$) in column content and solving for M at selected values of range R.

The regions of acceptable NO_2 concentration measurements ($\Delta M/M < 20\%$) are shown in Figure 6. The region enclosed by the curve A bounded by 1.1 ppm, 45 ppm, 100 m, and 400 m is that region in which NO_2 concentration can be measured to within 20% accuracy or less using the set of conditions assumed earlier.

The increase in the region of acceptable accuracy caused by increasing the absorption at the peak and decreasing the absorption at the minimum by a factor of five is shown by curve D bounded by 11 ppm, 0.7 ppm, 100 m, and 1000 m. Another means of enhancing the range of detectable concentrations is to extend the integration (or detection gate) time. The results of enhancement of this nature by an order of magnitude is illustrated by the increased region of detectability outlined by curve B. Further improvements can be obtained by increasing the laser power by an order of magnitude as shown by curve C. Improvement of curve C over Curve B is caused by the background which remains constant with a power increase but increases with increased gate time or number of pulses.

Now we can consider viable alternatives to improve the design of the system. Increasing power as opposed to increasing gate time (or averaging over a large number of pulses) is advantageous because of background interaction. There is also support for seeking a narrow linewidth laser if the more resolved structure produces increased absorption coefficient differences. In addition, narrow linewidth filters compatible with a narrower laser linewidth will decrease background when background is a limiting factor. However, the laser output energy per shot decreases as linewidth is narrowed indicating that an optimum combination is reached when laser energy losses due to narrowing become greater than the increase in absorption coefficient difference ($\Delta\alpha$).

B. Ozone Concentration in a Jet Wake at 20 km Altitude

In this section the DAS technique is analyzed for feasibility of detecting a depleted region of O_3 due to a catalytic reaction by NO_x in the wake of a jet engine. The catalytic reduction of O_3 by NO_x, identified by Johnston[19] in 1971, can be a detrimental result of SST operation in the stratosphere.

The consequence of such an occurrence would be an increase in ultraviolet sunlight intensity at the earth's surface since ozone is a very effective ultraviolet filter.

Consider a remote laser DAS system operating from an aircraft or balloon as illustrated in Figure 7. Assume an ambient O_3 concentration of 16×10^{-8} atm or 2 ppm (at 20 km the atmospheric density is .079 atm), a Rayleigh scattering coefficient of .01 km^{-1} at 300.0 nm (Figure 8) and 5.57×10^{3} km^{-1} at 347.2 nm (Figure 9), a backscatter factor[16] of .12 sr^{-1}, a detection efficiency of .05, detector gate time of .16 μsec (25 m range cells) and a telescope diameter of .25 m. The scattering coefficients given in Figures 8 and 9 are discussed in more detail in the following subsection. The lasers are assumed to have 1 joule per pulse at 300.0 nm and 347.2 nm for which O_3 absorption coefficients are $10.8(\text{atm cm})_e^{-1}$ and $.014(\text{atm cm})_e^{-1}$, respectively. The jet wake is assumed to be 100 m wide located at a range of 500 m from the observation platform as shown in Figure 7. Substituting the above parameters into Equation (3) the number of photons received at the detector from each range cell are calculated and listed in columns 3 and 4 of Table 1. The uncertainty in number density of O_3 for 25 m and 100 m range cells are listed in columns 5 and 6 respectively. The results show that O_3 concentrations of 5.4×10^{-8} atm to 8.9×10^{-8} atm can be detected using the 25 m range cells. The precision can be increased to 8.0×10^{-9} to 1.0×10^{-8} as noted in column 6 by using 100 m range cells. Although we increase precision by using 100 m range cells there is a corresponding loss in spatial resolution of locating concentration changes. Inclusion of particulates in the model would not significantly improve feasibility since it is not weak signal limited.

The conclusions to be derived from Table 1 then are that in monitoring O_3 concentration in a jet wake a decrease in the O_3 concentration by factors 3 to

10 can be observed under the simulated conditions. It should also be noted, however, that increasing the absorption cross section by using shorter wavelengths [(e.g., $\sigma_a \simeq 300$ (atm cm)$_e^{-1}$ at 250.0 nm] would also increase the precision of such a measurement. A considerable decrease in return signal n_{1j} can be tolerated without increasing the noise appreciably since n_{1j} is so large as shown in Table 1. In a recent calculation Brockman and Seals[21] determined that a two ended absorption measurement in the infrared with a tunable diode laser provides sensitivities of .02 to .2 ppm over 10 m for O_3, CO, NO, H_2O, and SO_2 with minimal interference effects. This result corresponds to a sensitivity of 1 to 10% of ambient for 10 m resolution which is more sensitive than the sensitivity of 50% to 6% calculated here for 25 m to 100 m resolution, respectively. The DAS technique does allow the measurement to be performed remotely rather than flying through the wake as required by a two-ended absorption measurement and DAS provides ranging information.

C. Ozone Measurements from an Orbiting Shuttle

The schematic arrangement considered for ozone profile measurements from an orbiting shuttle at 185 km altitude is shown in Figure 10. The 15-km deep ozone peak above 15 km in Figure 10 corresponds to the peak of the ozone concentration shown in Figure 11 as determined for the Midlatitude Summer Model Atmosphere.[16]

A scattering length of 4 km corresponding to a gate time of 26.67 microseconds is applied to the observed photomultiplier signal. The 4-km deep scattering lengths vary from 5 km to 45 km altitude at 4-km intervals. The ozone absorption cross sections used for the calculations shown in Figure 13 were measured by Griggs[20] with a resolution of .2 nm.

To perform sample calculations only Rayleigh scattering as obtained from "Optical Properties of the Atmosphere (Revised)"[16] is used for the backscattering medium of this DAS simulation. Consider the wavelengths of 300.0 nm (doubled dye laser and 347.2 nm (doubled ruby laser) as the laser wavelengths for strong 10.8 $(\text{atm cm})_e^{-1}$ and weak 0.014 $(\text{atm cm})_e^{-1}$ O_3 absorption, respectively. Using the Rayleigh scattering data for Midlatitude Summer at 337.1 nm and correcting with λ^{-4} the scattering coefficients and integrated scattering coefficient at 300.0 nm and 347.2 nm are calculated and plotted in Figure 8 and Figure 9, respectively. The backscatter β_{ij} as obtained from McClatchey, et al.[16] is .12 sr^{-1} of the scattering coefficient ξ_1 at range R (altitude h). Each laser pulse is considered to have 1 joule of energy. The combined efficiency of the optics and photomultiplier is considered to be 5%. The diameter of the receiver telescope is assumed as 1 m. The uncertainties reported here do not include multiple pulse averaging. Using the conditions defined above and values of $\int_o^{R_j} \xi_i(r)\, dr$ from Figure 9 and Figure 10 the predicted return signal is calculated with Equation (4) at 4-km intervals for each wavelength as listed in Table 2.

The predicted standard deviations (uncertainties) on column content are calculated using Equation (9) and listed in Table 2. These results are also plotted on Figure 13 as error bars on the assumed distribution of column content as seen from the shuttle to various range cell altitudes. Note that the predicted uncertainty, which is a measure of predicted sensitivity comparable to the inverse of signal-to-noise, increases from 3.0 m atm cm at 42 km to 8.0 m atm cm at 6 km. The percentage standard deviation is greater than 100% at 46 km and decreases to a minimum value of 2% at 22 km then increases to 3% at 6 km altitude. The percentage standard deviation is dominated by the distribution

of the column content M being measured; however, for evaluating techniques of measuring ozone content of the atmosphere it is the more important term to evaluate.

The standard deviations in ozone concentration are evaluated with Equation (10) and listed in Table 2 as ΔN and plotted as predicted error bars on Figure 11. The result yields an uncertainty of 13 (relative to 13) atm at 44 km (or 100%) then diminishes to 7 (out of 89) atm (or 8%) at 32 km then increases again to 25 (out of 53) atm (or 47%) at 12 km altitude. From the signal return strengths n_{1j} and n_{2j} of Table 2 it is apparent that the precision limitation in the upper atmosphere is limited by the amount of backscattering obtained whereas at lower altitudes attenuation at the strongly absorbed wavelength drives up the standard deviation. It is apparent from the n_{2j} return signal that the R^2 loss is more than compensated for by the increased backscatter caused by increasing air density.

The solutions presented assume no background fluctuations ($\delta n_{iB} = 0$), no detector noise ($\delta n_{iD} = 0$) and no amplifier noise ($\delta Q/Q = 0$). These preliminary calculations were performed on a programmable desk top calculator with limited capacity. The equations are being coded onto a large computer subsequent to which a variety of such problems will be analyzed for feasibility including all uncertainty estimates. Indications are that the noise terms included here are the dominant ones.

Results of the analysis at this point support the feasibility of monitoring the ozone profile from a shuttle. Some situations under consideration for future analysis include double peaked ozone distributions, a terminated signal return due to clouds, and total column contents of such gases as SO_2 and NO_2.

VI. CONCLUSIONS

The analysis technique presented in this report is capable of predicting the sensitivity attainable with a specified lidar system for a given atmospheric model using Differential Absorption and Scattering. Such calculations are necessary for determining feasibility of developing the technique for a given application and for estimating design parameters of a DAS Lidar system. Capabilities of the DAS technique for three applications have been analyzed and can serve as initial design criteria.

The analysis of horizontal NO_2 concentration measurements indicates that the proposed system can measure average NO_2 concentrations (or column contents) to 400 m over a concentration range of 1.1 to 40 ppm to within 20%, which is in the region of interest of the recommended threshold level of 5 ppm.[22] The design parameters analyzed in this report indicate that in order to monitor ambient NO_2 concentrations in a range of .01 to .2 ppb[23] lasers of considerably more energy than .75 mj per pulse and/or integration times of much greater than 10 ns are required. In addition, the return signals can be interpreted to indicate whether an out of range measurement (>20% predicted standard deviation) is above or below the concentrations allowed for reasonable errors.

The analysis of ozone concentration in a jet wake at 20 km indicates that a drop to about 30% of ambient can be detected which is sufficient to indicate the presence of the wake and thus determine its persistence and spread with time. The analysis of an ozone profile measurement from shuttle at 185 km has shown that for the system described we can expect to determine ozone concentration to within 10% at the peak (h = 22 km) and 68% at 8 km and 41 km with concentrations at altitudes between 14 and 40 km being measurable to within a precision between 6.3% and 36%. The same system analyzed for total burden to the satellite measurements is predicted to have a precision range of 2% at 17 km to 11% at 38 km with all precisions below 38 km being less than 11%.

The next step is to include interference effects from other molecular gases that have absorption structure within the wavelengths used for the measurement based on an approximate model of gas distribution over the intended absorption path of the measurement. The analysis has been based on a photon counting system and neglects statistical errors caused by amplifier gain when large count rates are encountered. The calculations are being expanded to include these sources of error. In a similar fashion, this evaluation technique can be extended to infrared systems where photon counting is not possible.

Table 1. Ozone Density, Estimated Signal Returns, and Predicted Uncertainty for Ozone Concentrations as a Function of Range for Jet Wake Concentration Measurements.

Range (m)	O_3 Density (10^{-8} atm)	N_1 (3000) (counts)	N_2 (3472) (counts)	ΔN_{O_3} (10^{-9} atm) ΔR = 25 m	ΔN_{O_3} (10^{-8} atm) ΔR = 100 m
400	16	576076	437790	5.4	
425	16	505653	387686		
450	16	446926	345704		
475	16	397470	310179		.81
500	8	356992	279856		
525	0	323640	253765		
550	0	294740	231154	7.1	
575	0	269532	211430		
600	8	246349	194122		.98
625	16	224970	178850		
650	16	206105	165308	8.9	
675	16	189382	153244		

Other Pertinent Parameters

$\eta = .05$

$E = 1$

$T = .16 \times 10^{-6}$ sec

$d = .25$ m

$\lambda_1 = 3000 \times 10^{-10}$ m

$\beta_1 = 1.0 \times 10^{-5}\ m^{-1} \times .12$

$\xi_1 = 1.0 \times 10^{-5}\ m^{-1}$

$\sigma_1 = 10.8\ atm^{-1}\ cm^{-1}$

$\lambda_2 = 3472 \times 10^{-10}$ m

$\beta_2 = 5.7 \times 10^{-6}\ m^{-1} \times .12$

$\xi_2 = 5.7 \times 10^{-6}\ m^{-1}$

$\sigma_2 = .014\ atm^{-1}\ cm^{-1}$

Table 2. Calculated values of received signal strength on resonance absorption (n_{1j}), received signal strength off resonance absorption (n_{2j}), predicted standard deviation in ozone column content (δM) and predicted standard deviation in ozone concentration (δN) as functions of range (R) from the shuttle.

Altitude h(km)	Range R_j(km)	n_{1j} (Photons per range cell)	n_{2j} (Photons per range cell)	M (matm cm)	δM (matm cm)	$\langle N \rangle_j$ (n atm)	δN (n atm)
6	179	22	18829	316	9		
8	177					47	31
10	175	36	17852	297	7		
12	173					53	25
14	171	48	13515	276	6		
16	169					76	22
18	167	62	8532	245	5		
20	165					128	18
22	163	115	5095	194	4		
24	161					169	12
26	159	299	3029	126	2		
28	157					128	8
30	155	555	1847	75	2		
32	153					89	7
34	151	695	1064	39	2		
36	149					54	8
38	147	641	613	18	2		
40	145					28	10
42	143	470	352	6	3		
44	141					13	13
46	139	302	202	1	4		

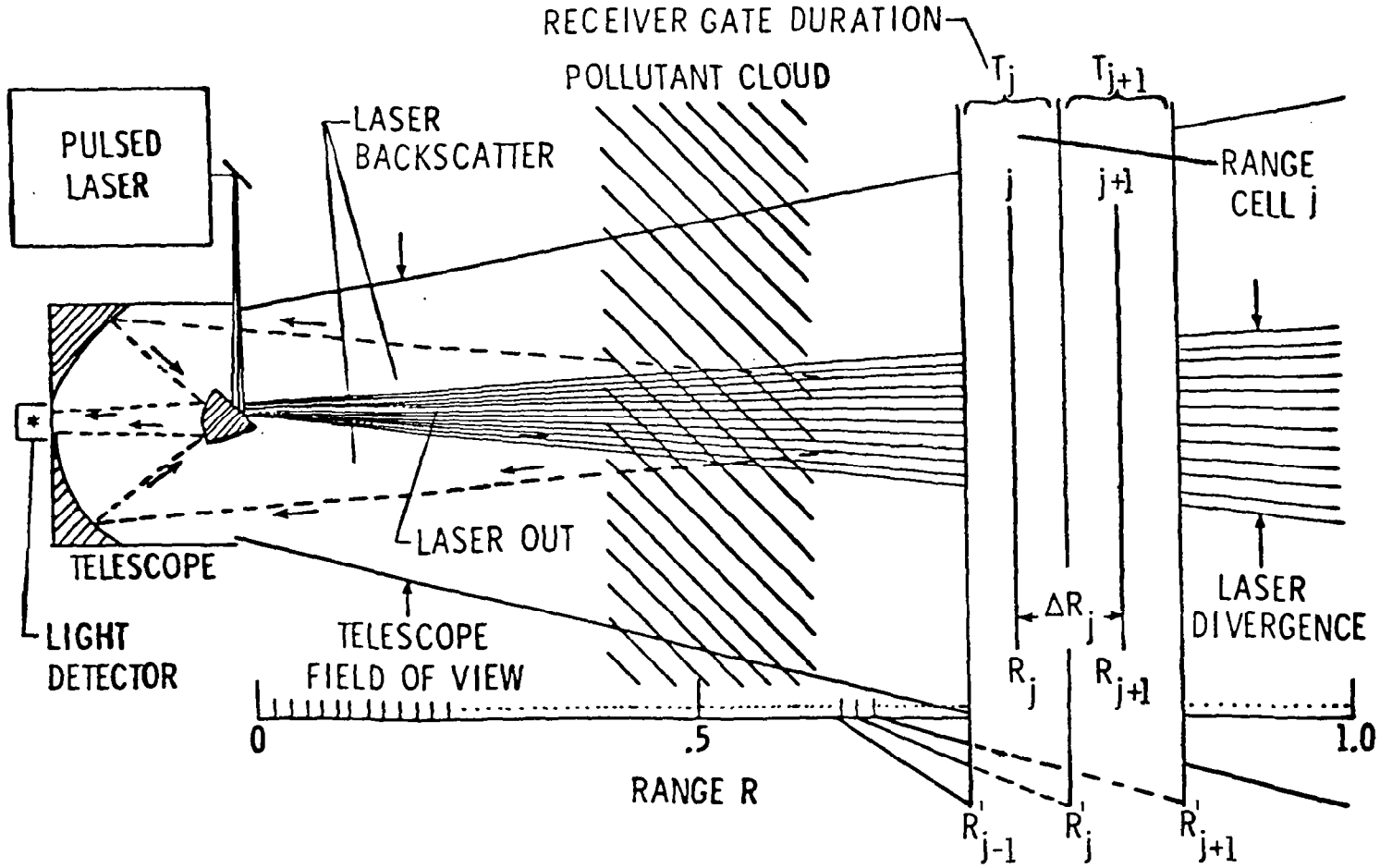

Figure 1. Simplified diagram of the Differential Absorption and Scattering (DAS) LIDAR Technique.

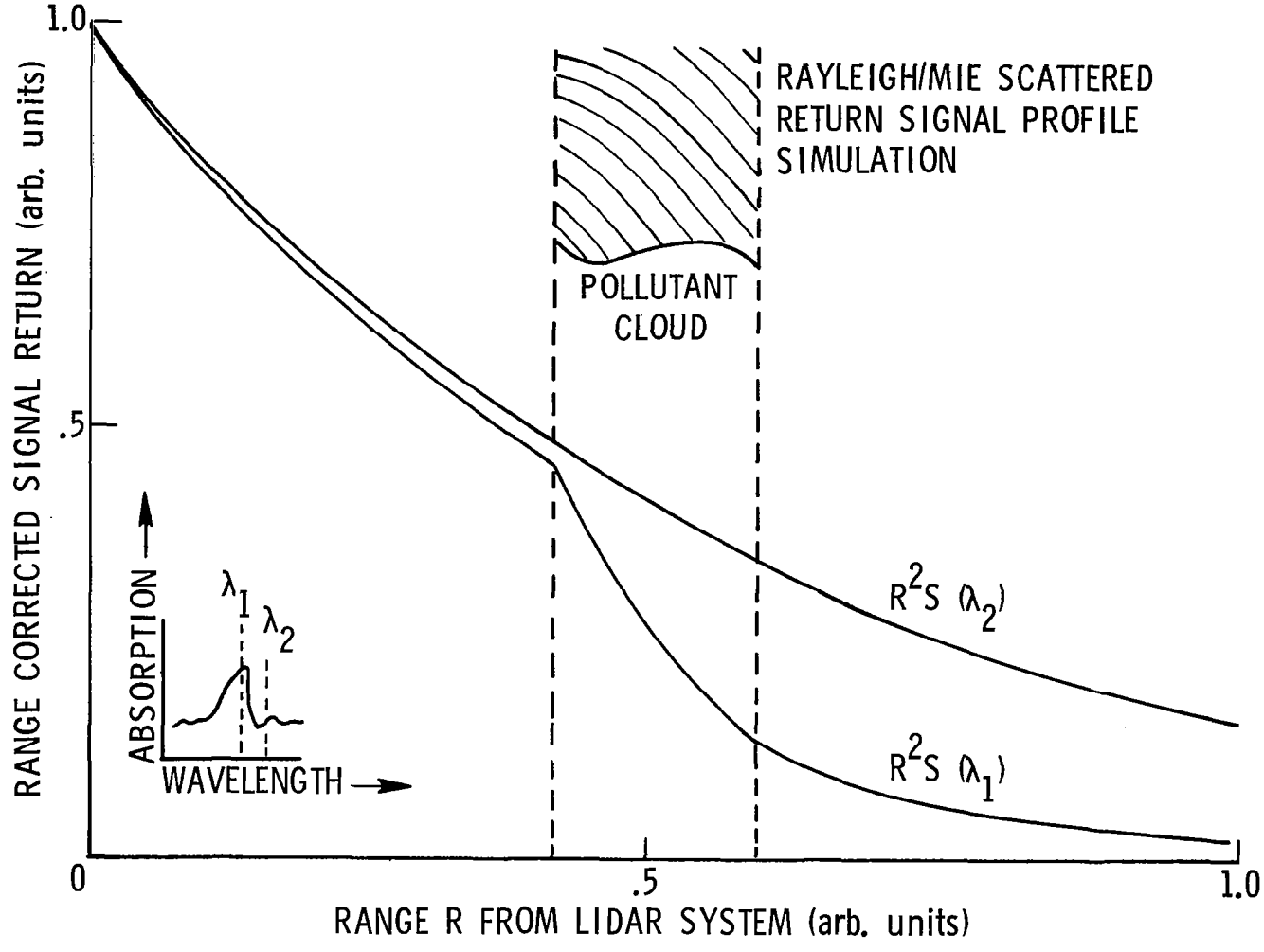

Figure 2. Simulated two-wavelength signal strength received from a DAS LIDAR system as described in Figure 1.

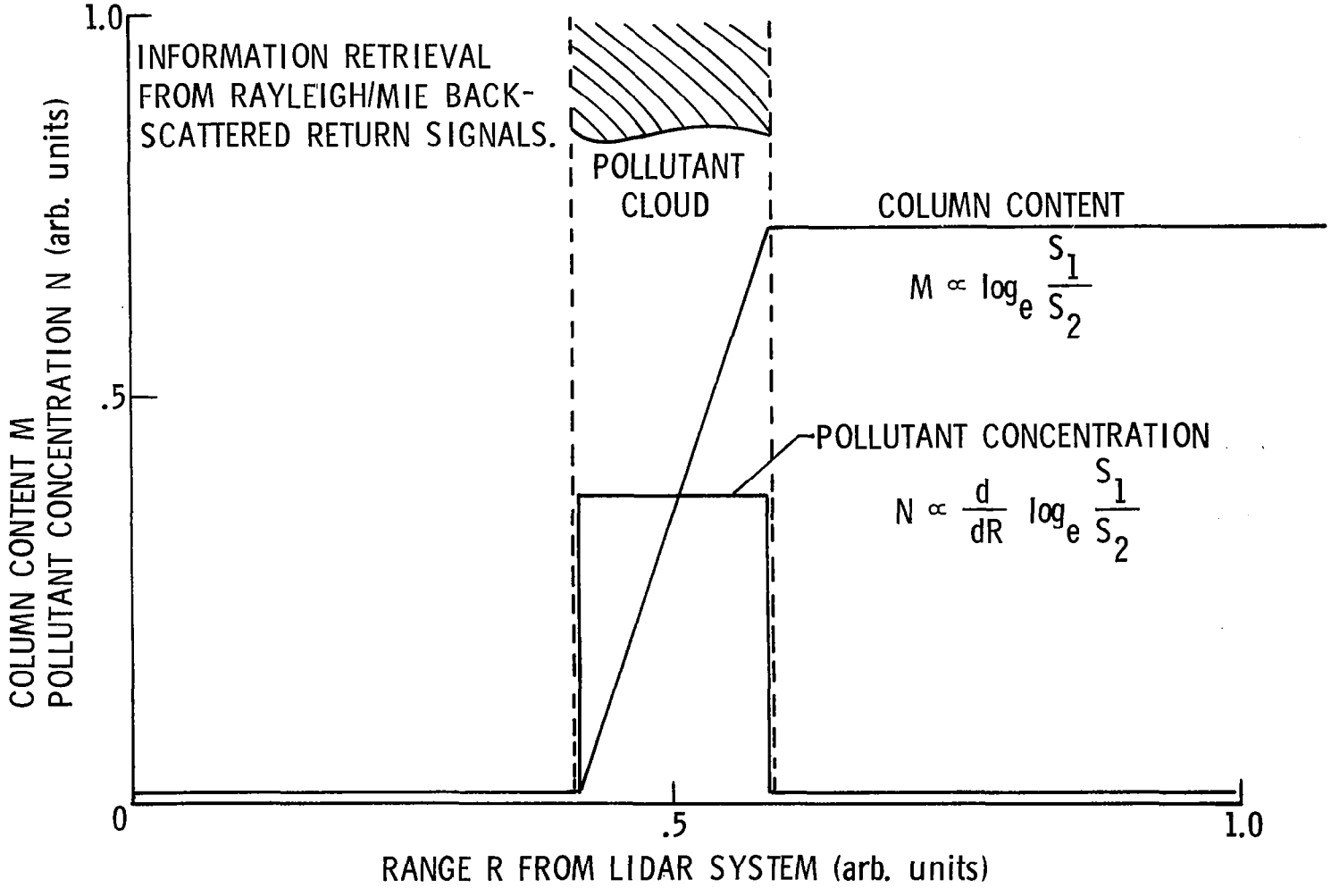

Figure 3. Simulated results from processed DAS LIDAR return signals shown in Figure 2.

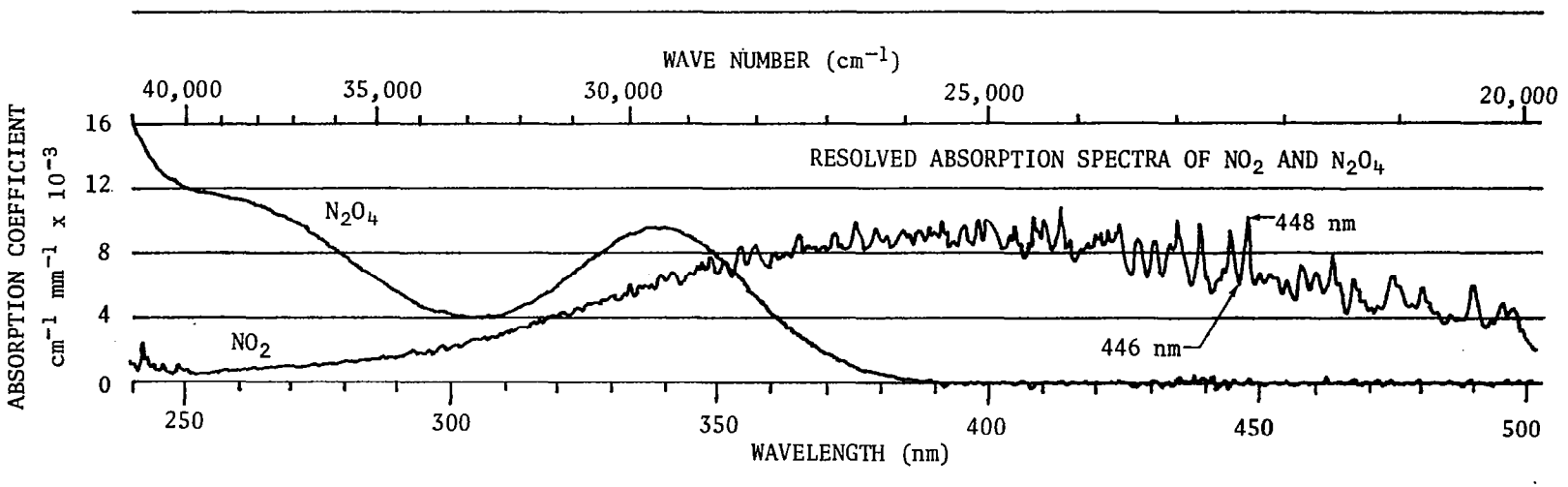

Figure 4. Absorption coefficients of NO_2 and N_2O_4 vs wavelength measured at 25°C by Hall and Blacet.[18]

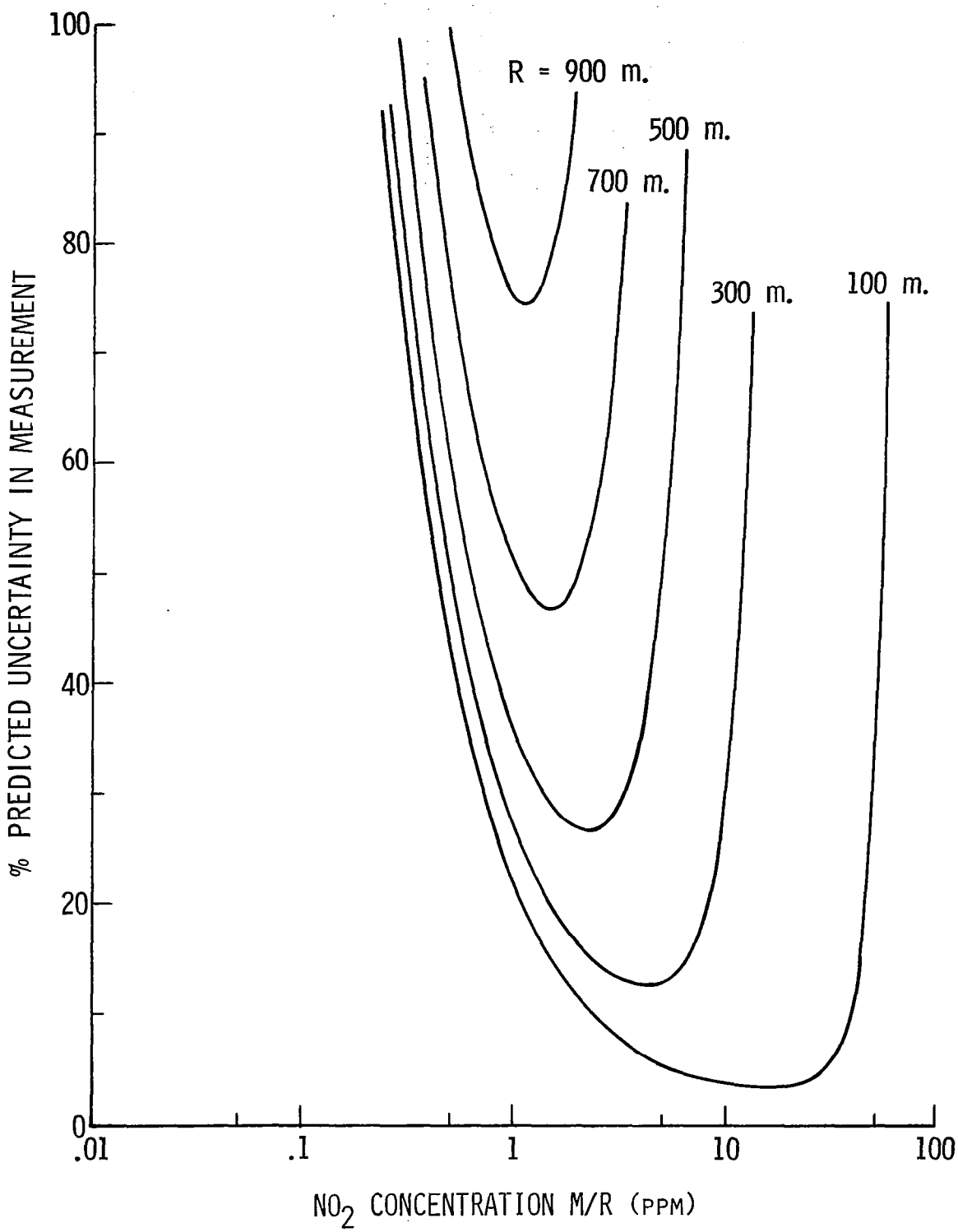

Figure 5. Predicted uncertainty in NO_2 average concentration measurements by DAS as a function of concentration at various ranges from the detector.

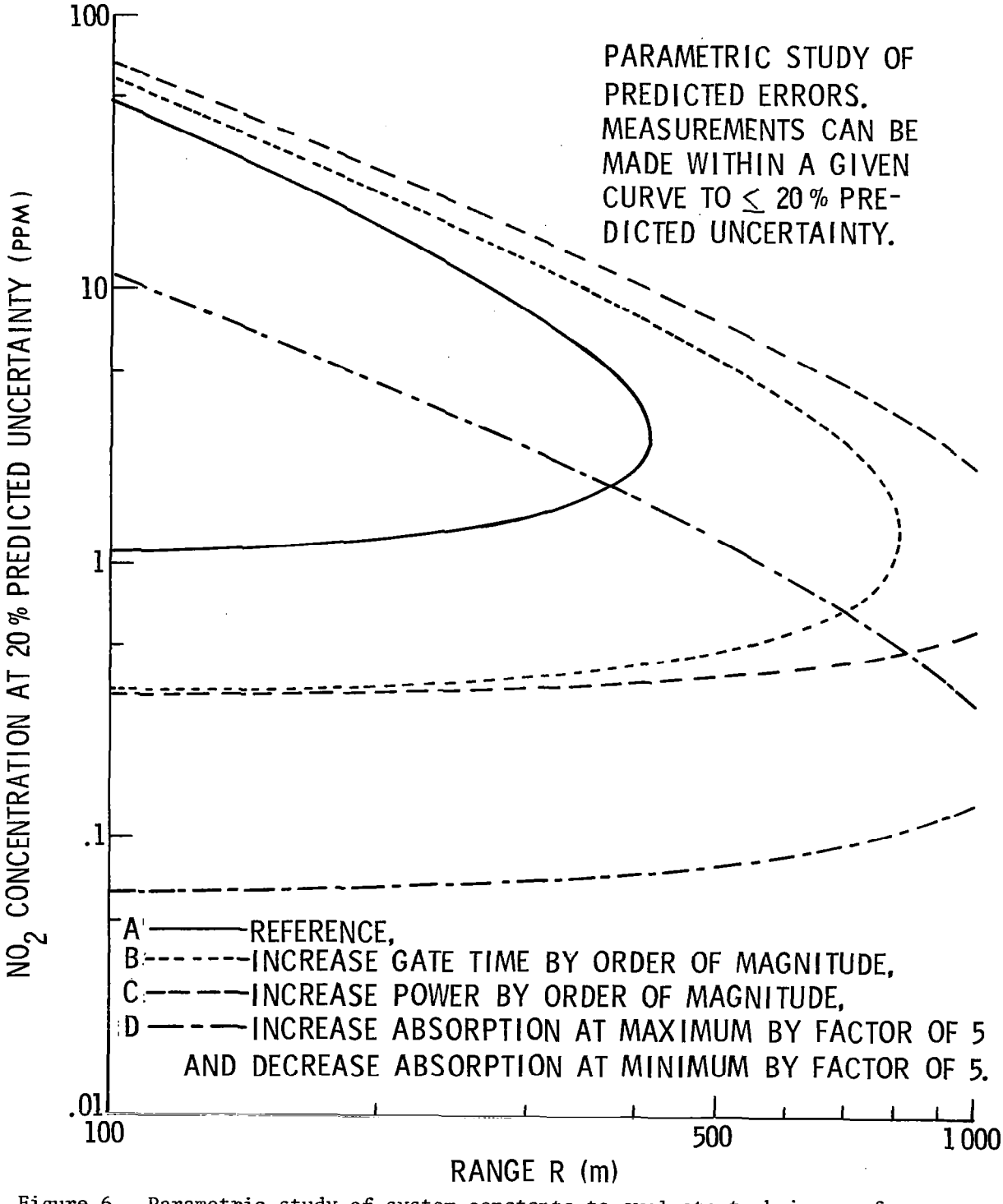

Figure 6. Parametric study of system constants to evaluate techniques of enhancement for NO_2 concentration measurements by DAS.

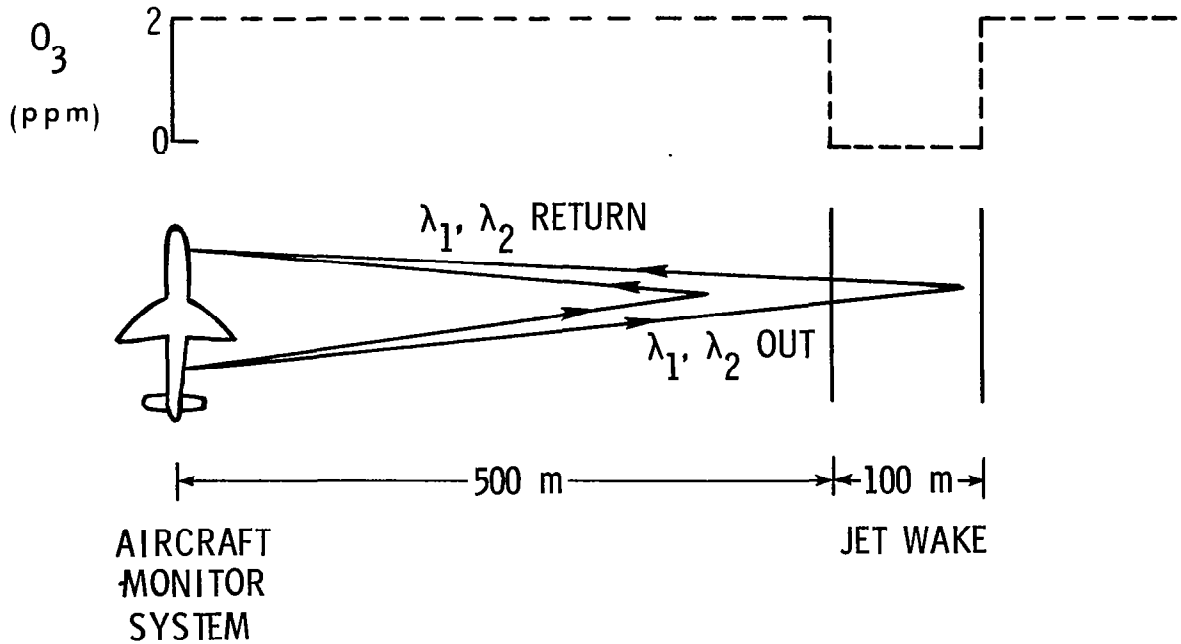

Figure 7. System schematic to monitor ozone depletion at SST altitudes from an aircraft using DAS LIDAR.

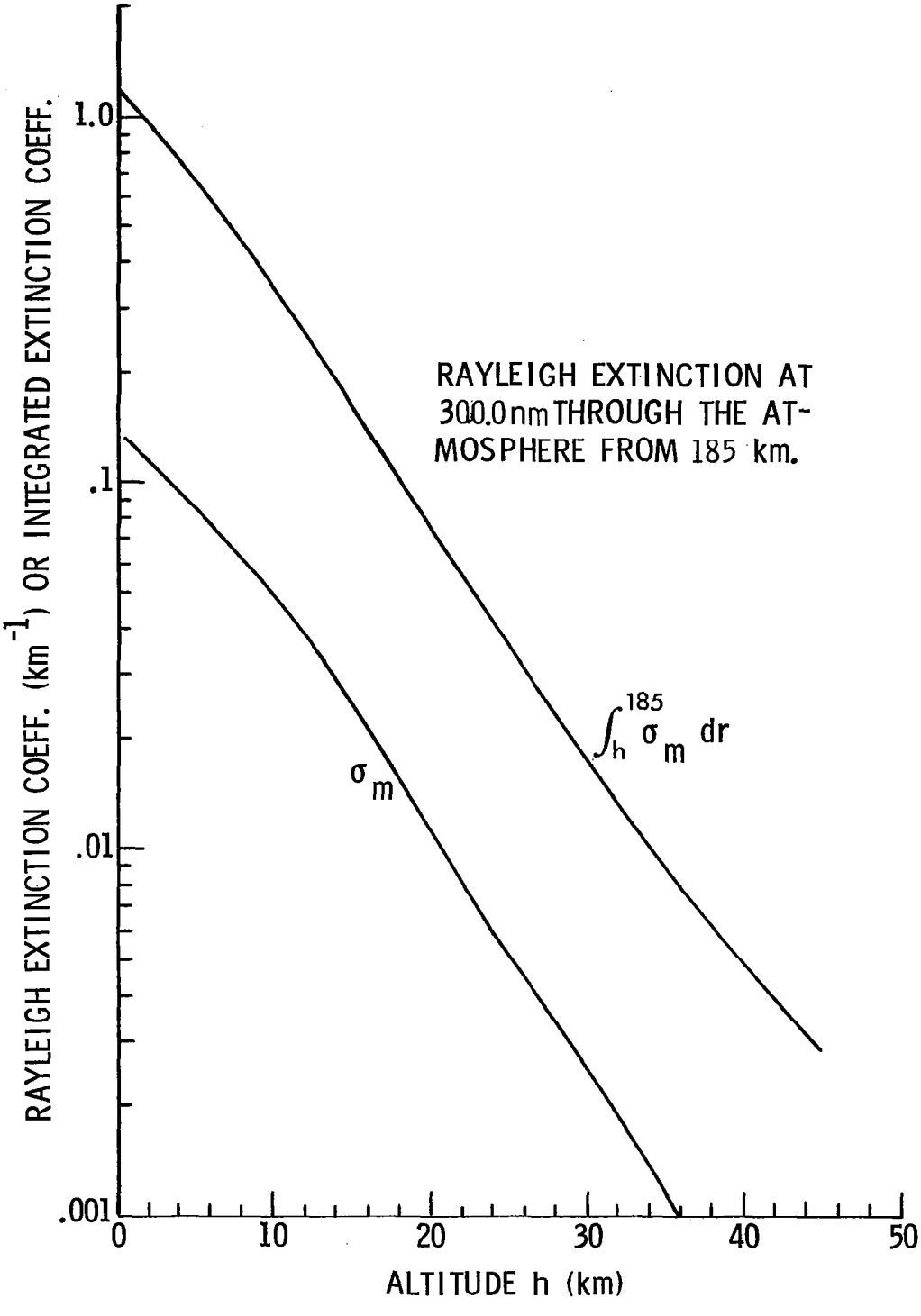

Figure 8. Rayleigh extinction coefficients and integrated extinction coefficients at 300.0 nm plotted as a function of altitude but observed from the NASA shuttle.

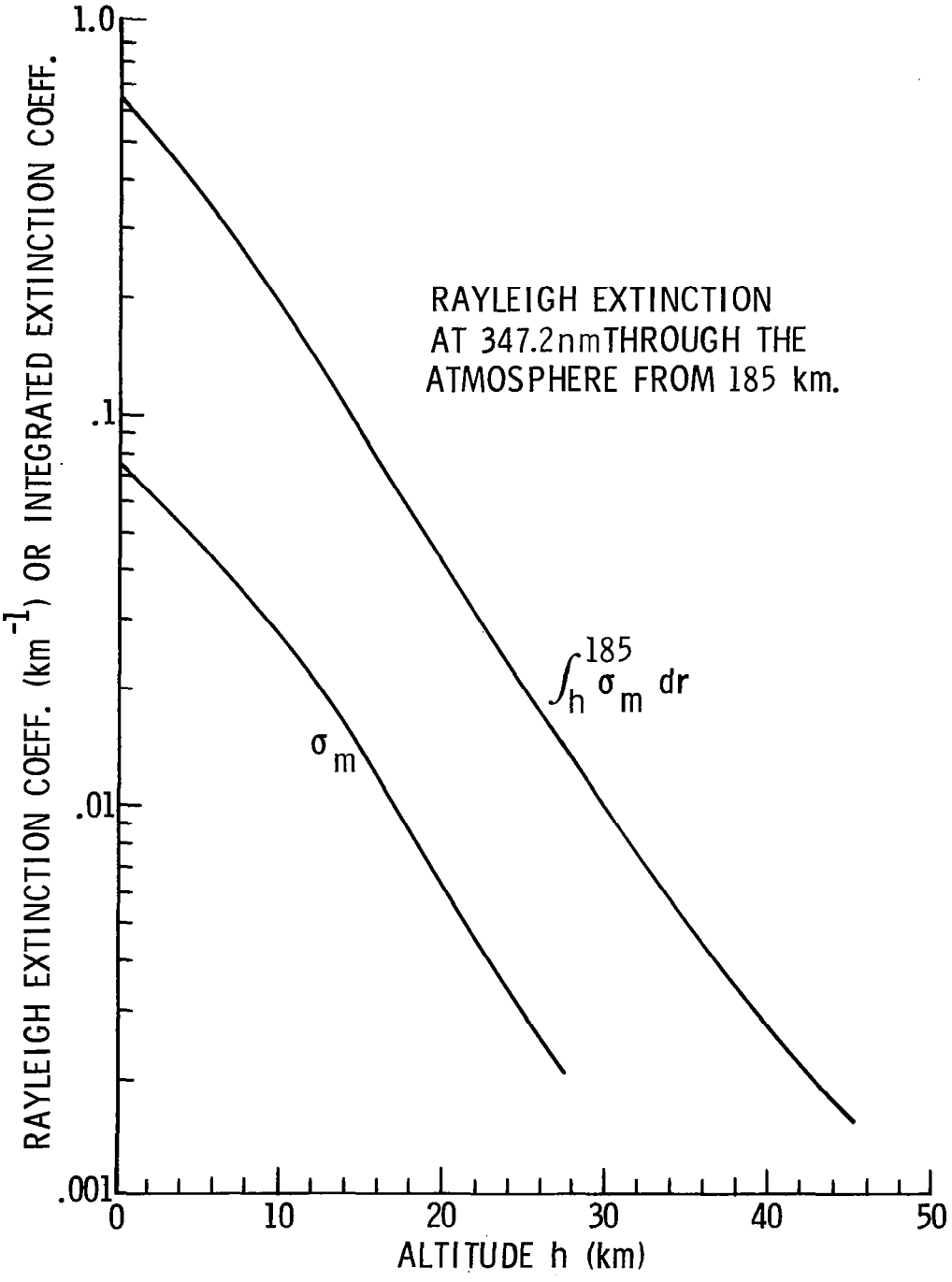

Figure 9. Rayleigh extinction coefficients and integrated extinction coefficients at 3472 nm plotted as a function of altitude but observed from the NASA shuttle.

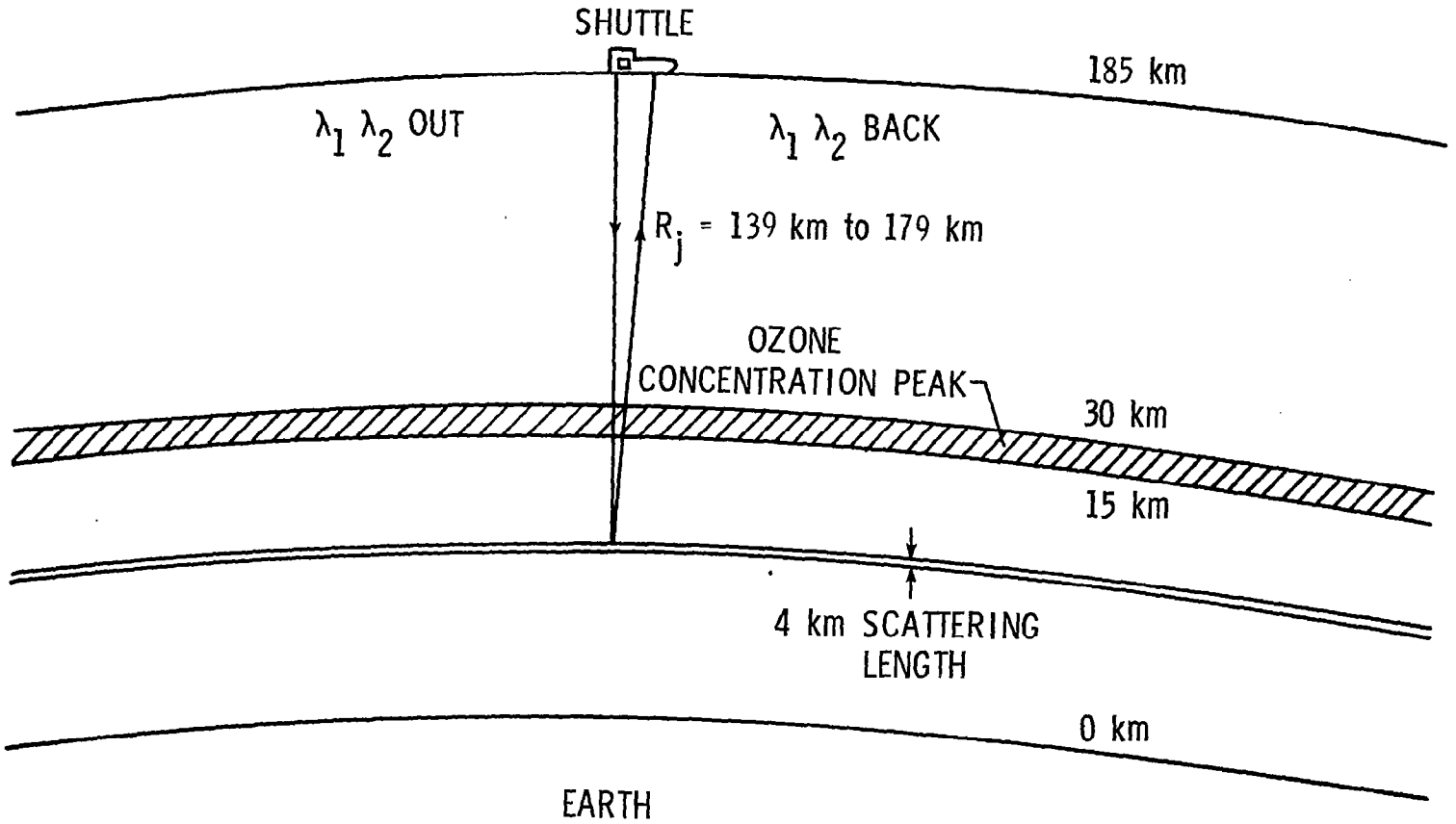

Figure 10. Model used for predicted uncertainty calculations of DAS ozone concentration measurements from the shuttle.

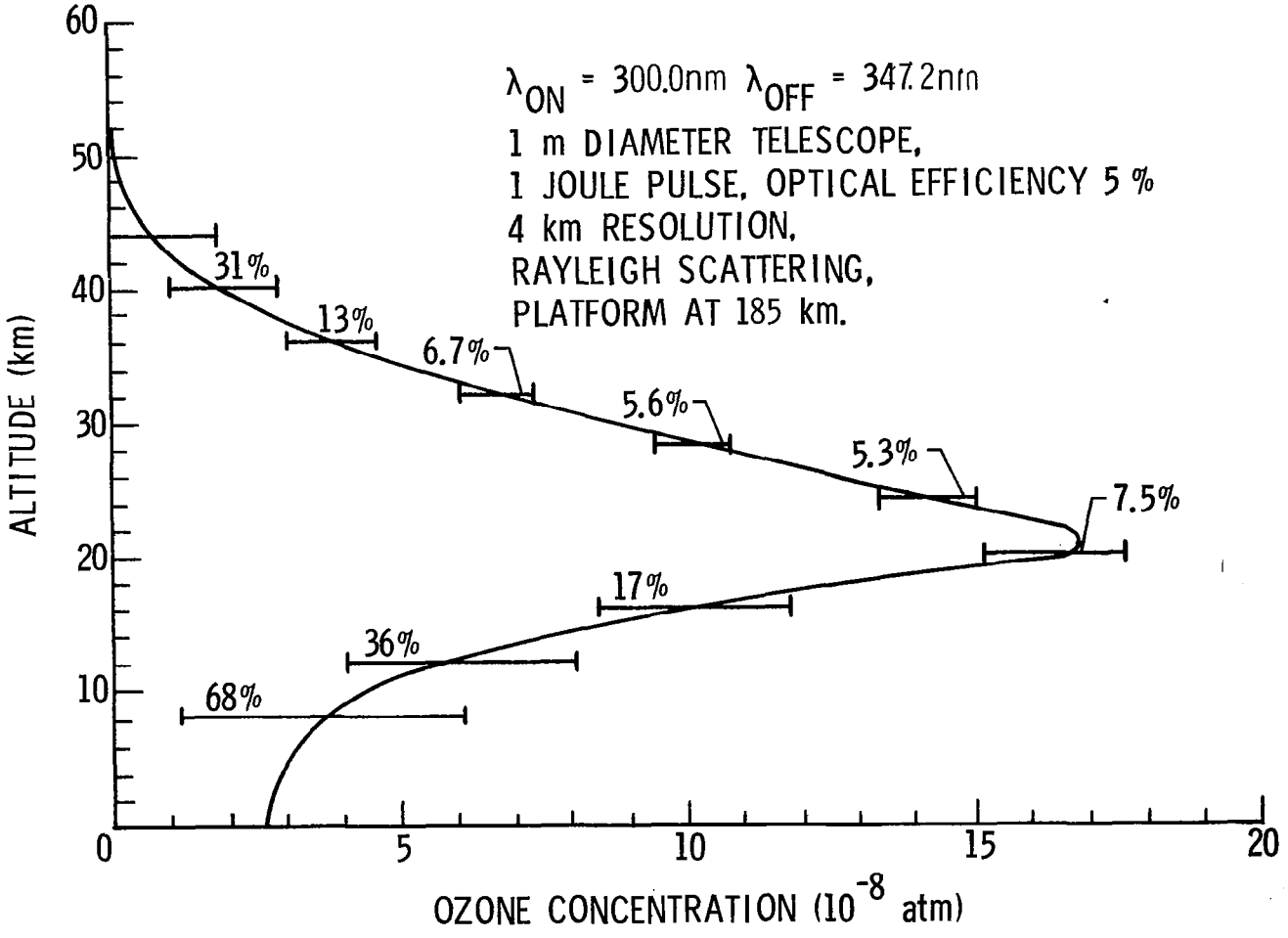

Figure 11. Predicted uncertainties as calculated for ozone concentration measurements performed from the NASA shuttle.

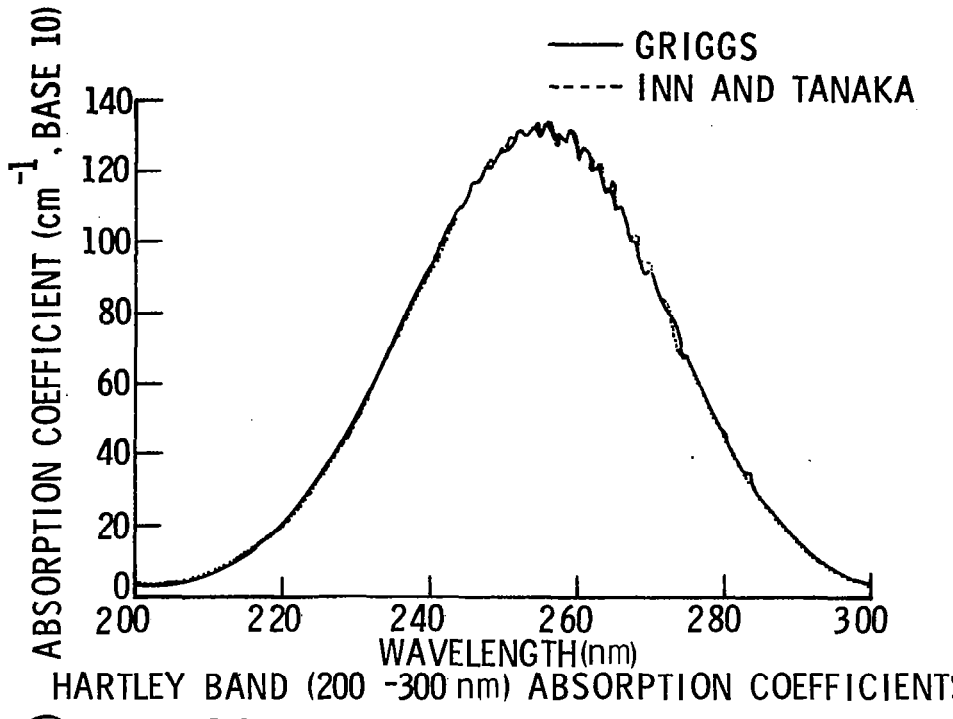

HARTLEY BAND (200 -300 nm) ABSORPTION COEFFICIENTS.

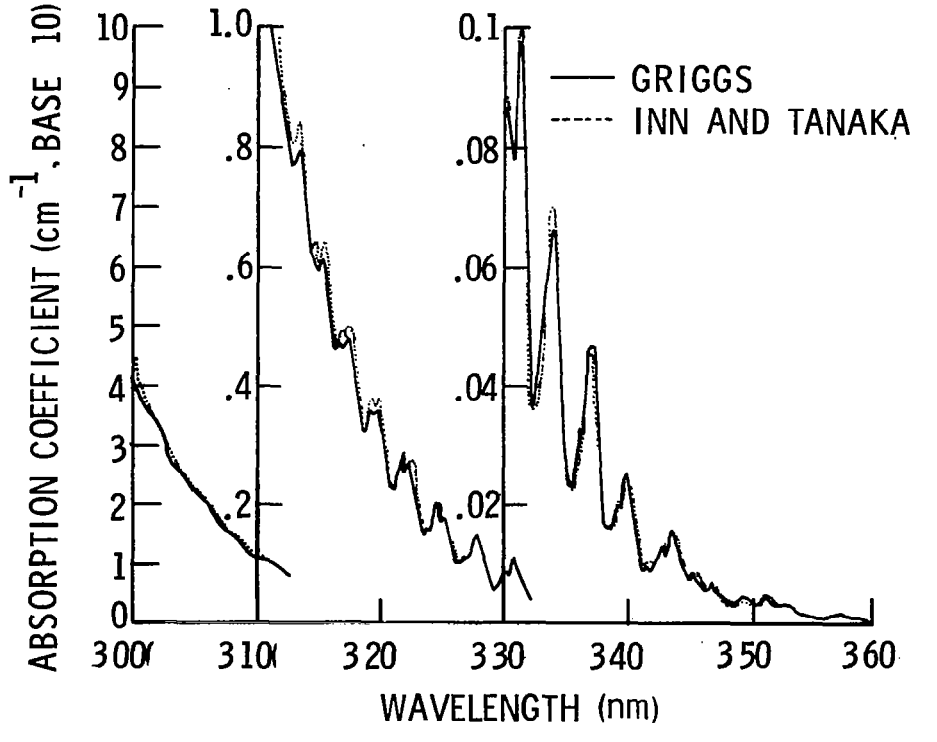

HUGGINS BAND (300 -360nm)
ABSORPTION COEFFICIENTS.

Figure 12. Ozone absorption coefficients vs wavelength reported by Griggs.[20]

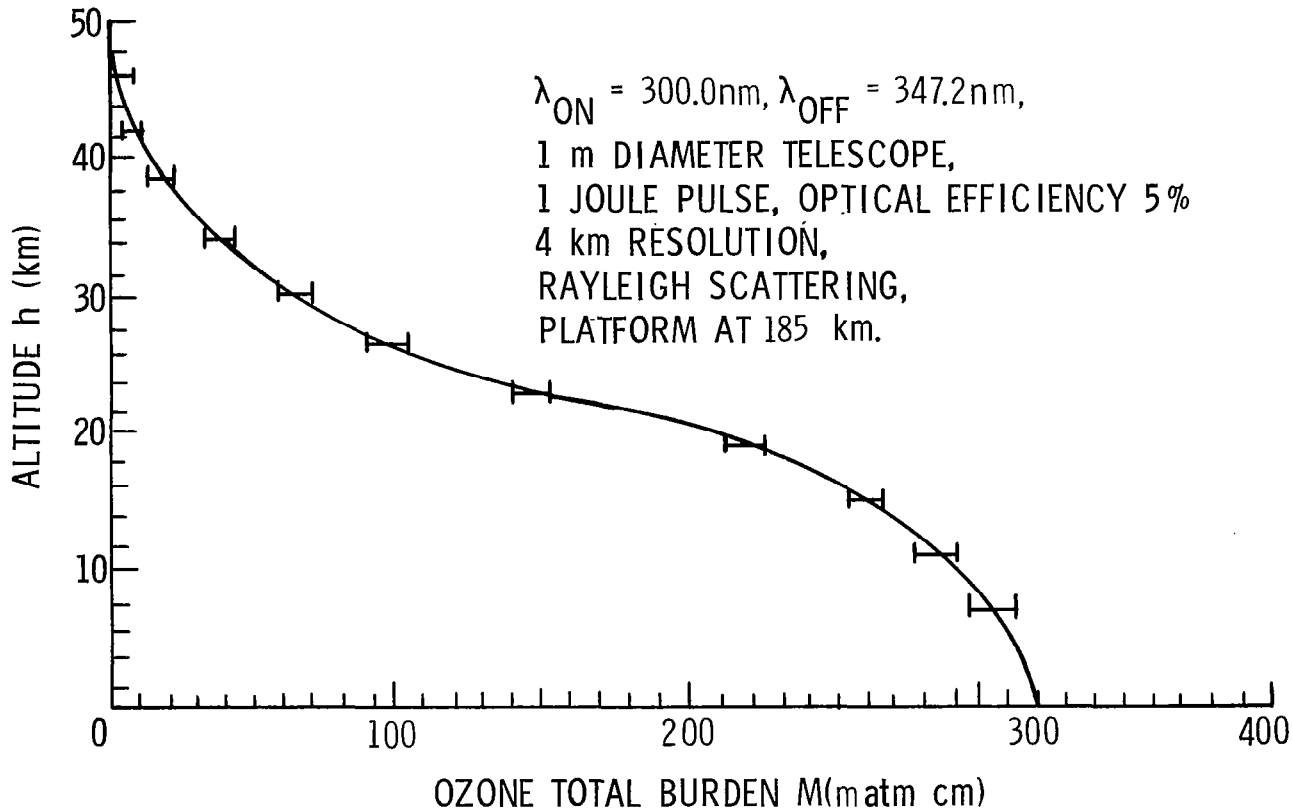

Figure 13. Predicted uncertainties as calculated for ozone column content measurements to various altitudes from the NASA shuttle.

REFERENCES

[1] Schotland, R. M.: Some Observations of the Vertical Profile of Water Vapor by Means of a Laser Optical Radar. Proceedings of the Fourth Symposium on Remote Sensing of Environment. April 12-14, 1966, Ann Arbor, Michigan. pp. 273-283.

[2] Measures, R. M.: A Comparative Study of Laser Methods of Air Pollution Mapping. UTIAS Report No. 174, University of Toronto, Canada (1971).

[3] Measures, R. M.; and Pilon, G.: A Study of Tunable Laser Techniques for Remote Mapping of Specific Gaseous Constituents of the Atmosphere. Opto-Electronics, vol. 4, 141-153 (1972).

[4] Kildal, H.; and Byer, R. L.: Comparison of Laser Methods for the Remote Detection of Atmospheric Pollutants. Proceedings of the IEEE, vol. 59, no. 12, 1644-1663 (1971).

[5] Byer, R. L.; and Garbuny, M.: Pollutant Detection by Absorption Using Mie Scattering and Topographical Targets as Retroreflectors. Applied Optics, vol. 12, no. 7, 1496-1505 (1973).

[6] Schotland, R. M.: Errors in the Lidar Measurement of Atmospheric Gases by Differential Absorption. Journal of Applied Meteorology, vol. 13, 71-77, (1974).

[7] Ahmed, S. A.: Applied Optics, vol. 12, 901-904 (1973).

[8] Bevington, P. R.: Data Reduction and Error Analysis for the Physical Sciences. McGraw-Hill, New York (1969).

[9] Putley, E. H.: Solid State Devices for Infra-red Detection. Scientific Instruments, vol. 43, 857-868, (1966).

[10] Wolfe, W. L., Editor: Handbook of Military Infrared Technology, U. S. Government Printing Office, Washington, DC (1965).

[11] Knestrick, G. L.; and Curcio, J. A.: Measurements of Ultraviolet Spectral Radiance of the Horizon Sky. Applied Optics, vol. 9, no. 7, 1574-1576 (1970).

[12] Fenn, Robert W.: Correlation Between Atmospheric Backscatter and Meteorological Range. Applied Optics, vol. 5, 293-295 (1966).

[13] Elterman L.: Aerosol Measurements in the Troposphere and Stratosphere. Applied Optics, vol. 5, no. 11, 1769-1776 (1966).

[14] Elterman, L.: Relationships Between Vertical Attenuation and Surface Meteorological Range. Applied Optics, vol. 9, no. 8, 1804-1810 (1970).

[15] McCormick, M. P.: Simultaneous Multiple Wavelength Laser Radar Measurements of the Lower Atmosphere. Presented at the Electro-Optic International Conference, Brighton, England (1971).

[16] McClatchey, R. A.; Fenn, R. W.; Selby, J. E. A.; Volz, F. E.; and Garing, J. S.: Optical Properties of the Atmosphere (Revised). AFCRL-71-0279, Environmental Research Paper No. 354, Air Force Cambridge Research Laboratory, Bedford, Massachusetts (1971).

[17] NASA Langley Research Center, Remote Measurement of Pollution. NASA SP-285, National Technical Information Service, Springfield, VA.

[18] Hall, T. E., Jr.; and Blacet, F. E.: Separation of the Absorption Spectra of NO_2 and N_2O_4 in the Range 2400-5000 Å. The Journal of Chemical Physics, bol. 20, 1745-1749 (1952).

[19] Johnston, H. S.: Catalytic Reduction of Stratospheric Ozone by Nitrogen Oxides. Lawrence Radiation Lab. Report UCRL 20568, June 1971.

[20] Griggs, M. J.: Absorption Coefficients of Ozone in the Ultraviolet and Visible Regions. The Journal of Chemical Physics, vol. 49, no. 2, 857-859 (1968).

[21] Brockman, Philip; and Seals, R. K., Jr.: Analysis of Laser Measurement of High-Altitude Aircraft Emissions. AIAA Journal, vol. 12, no. 5., May 1974, pp. 651-655.

22 Sax, N.I.: Dangerous Properties of Industrial Materials. Reinhold Publishing Corp., New York (1963), p. 1042.

23 Williamson, S.J.: Fundamentals of Air Pollution. Addison Wesley Publishing Company, Inc., Reading, Massachusetts (1973), p. 379.